Design of Nonlinear Controllers for Active Vehicle Suspensions Using Parameter-Varying Control Synthesis [*]

Ian J. Fialho[†]
Dynacs Engineering - Boeing ISS
Houston, TX USA

Gary J. Balas
Department of Aerospace Engineering and Mechanics
University of Minnesota
Minneapolis, MN USA

July 19, 1999

---

[*] To Appear: Vehicle System Dynamics

[†] Corresponding Author: Boeing ISS, Mail Stop HS44; 2100 Space Park Drive; Houston TX 77058, USA; Email: ian.fialho@sw.boeing.com; Fax: (281) 336 5070

Abstract

Nonlinear suspension controllers have the potential to achieve superior performance compared to their linear counterparts. A nonlinear controller can focus on maximizing passenger comfort when the suspension deflection is small compared to its structural limit. As the deflection limit is approached, the controller can shift focus to prevent the suspension deflection from exceeding this limit. This results in superior ride quality over the range of road surfaces, as well as reduced wear of suspension components. This paper presents a novel approach to the design of such nonlinear controllers, based on linear parameter-varying control techniques. Parameter-dependent weighting functions are used to design active suspensions that stiffen as the suspension limits are reached. The controllers use only suspension deflection as a feedback signal. The proposed framework easily extends to the more general case where all the three main performance metrics, i.e., passenger comfort, suspension travel and road holding are considered, and to the design of road adaptive suspensions.

1 Introduction

Conventional passive suspensions that employ a spring and damper between the car body and wheel assembly, represent a tradeoff between conflicting performance metrics such as passenger comfort, road holding, and suspension deflection. Since the late sixties there has been considerable research into the use of feedback control to improve suspension design, i.e., active suspensions. This would be implemented by placing a hydraulic actuator, controlled by feedback, between the chassis and wheel assembly. The applications of active suspensions range from improved maneuverability in off-road vehicles [1], to better comfort/road holding tradeoffs in consumer automobiles, and superior handling of championship race cars [2]. Several control design methods have been used to design suspension control laws, notably linear optimal control [3, 4, 5, 6], nonlinear control [7, 8] and adaptive control [9]. Investigations have shown that active suspensions that focus on minimizing a fixed performance measure offer limited benefit over conventional passive ones and that the full potential of active suspensions can only be realized by exploiting their inherent adaptive capabilities (see [10, 3, 4] and the references therein). By adaptive we refer to the ability to emphasize different performance objectives depending on the current operating conditions, by on-line updating of controller parameters. For example, if the lateral accelerometers indicate operation on a straight road section the road holding performance requirement may be relaxed considerably.

In this paper we discuss the design of an active suspension system that adjusts its parameters depending on the amount of suspension travel, i.e., the relative displacement between the chassis and wheel assembly. Structural features of a vehicle place a hard limit on how large this displacement may be. Hitting this limit results in not only considerable passenger discomfort, but increases the wear of the vehicle. With current trends in automobile designs favoring lower hoods and larger tyres, this constraint is even more critical. Most earlier attempts to account for this hard constraint have involved incorporating it into a weighted quadratic performance index that is minimized using linear optimal control theory (see [3, 4] and the references therein). The weight on the suspension deflection is chosen so that even the most malevolent road inputs do not cause the suspension limits to be reached. The conservatism of this approach stems from the fact that in order to lower the vertical acceleration experienced by the car body, i.e., increase passenger comfort, larger suspension travel is required. Since the controller is linear, and is designed for worst-case road inputs, under normal road conditions insufficient suspension deflection is generated. As a consequence passenger comfort is lower than is possible with a nonlinear control law.

The above discussion was used in reference [8], to motivate the design of a nonlinear control law that focuses on passenger comfort, i.e., keeping vertical acceleration small, when the suspension travel is away from its limits. As the travel limits are approached the controller focuses on keeping the suspension travel small, thereby preventing the limit from being reached. The controller in reference [8] was designed using backstepping techniques [11] with full-state feedback, and the transition between a "soft" and "stiff" suspension was achieved by means of a novel nonlinear filter. Possible extensions of these ideas to road adaptive suspensions are described in [12].

In this paper we present an alternative framework in which the design of nonlinear suspension control laws can be carried out. More specifically, we use recent linear parameter-varying (LPV) control techniques (see [13, 14] and the references therein), to design control laws that stiffen as the suspension travel limits are reached. An overview of parameter-varying techniques is found in Section 2. In Section 3 we discuss fundamental limitations of linear control in achieving both passenger comfort and small suspension deflection. $\mathcal{H}_\infty$ controllers that emphasize either passenger comfort or suspension travel are the subject of Section 4. In Section 5 we use linear parameter-varying techniques to combine the above $\mathcal{H}_\infty$ designs into in a nonlinear controller that stiffens as the suspension deflection limits are reached. In Section 6 we discuss extensions of the above ideas to the more general case where all the three main performance metrics, i.e., passenger comfort, suspension travel and road holding are considered, and to the design of road adaptive suspensions. Concluding comments are found in Section 7.

2 Linear parameter-varying control design

We begin with a brief introduction to gain-scheduling based on linear parameter-varying (LPV) plant representations. For a compact subset $\mathcal{P} \subset \mathcal{R}^s$, the parameter variation set $\mathcal{F}_\mathcal{P}$ denotes the set of all piecewise continuous functions mapping $\mathcal{R}$ (time) into $\mathcal{P}$ with a finite number of discontinuities in any interval. The compact set $\mathcal{P} \subset \mathcal{R}^s$, along with continuous functions $A : \mathcal{R}^s \to \mathcal{R}^{n \times n}$, $B : \mathcal{R}^s \to \mathcal{R}^{n \times n_d}$, $C : \mathcal{R}^s \to \mathcal{R}^{n_e \times n}$ and $D : \mathcal{R}^s \to \mathcal{R}^{n_e \times n_d}$ represent an nth order linear parameter-varying (LPV) system $G_{\mathcal{F}_\mathcal{P}}$, whose dynamics evolve as

$$\begin{bmatrix} \dot{x}(t) \\ e(t) \end{bmatrix} = \begin{bmatrix} A(\rho(t)) & B(\rho(t)) \\ C(\rho(t)) & D(\rho(t)) \end{bmatrix} \begin{bmatrix} x(t) \\ d(t) \end{bmatrix}, \quad \rho \in \mathcal{F}_\mathcal{P}. \tag{1}$$

The system in equation (1) is said to be quadratically stable if there exists a matrix $X = X^T > 0$ such that

$$A^T(\rho)X + XA(\rho) < 0,$$

for all $\rho \in \mathcal{P}$. It is well known that if the system (1) is quadratically stable then it is exponentially stable for any parameter trajectory $\rho(\cdot) \in \mathcal{F}_\mathcal{P}$. The induced $\mathcal{L}_2$ norm of a LPV system $G_{\mathcal{F}_\mathcal{P}}$, with zero initial conditions, is defined as

$$\|G_{\mathcal{F}_\mathcal{P}}\| \doteq \sup_{\rho \in \mathcal{F}_\mathcal{P}} \; \sup_{\| d\|_2 \neq 0, d \in \mathcal{L}_2} \frac{\|e\|_2}{\|d\|_2}. \tag{2}$$

It is well known that if $G_{\mathcal{F}_\mathcal{P}}$ is quadratically stable then this quantity is finite.

From the point of view of control design we assume that the plant has the partitioned LPV representation,

$$\begin{bmatrix} \dot{x}(t) \\ e(t) \\ y(t) \end{bmatrix} = \begin{bmatrix} A(\rho) & B_1(\rho) & B_2(\rho) \\ C_1(\rho) & D_{11}(\rho) & D_{12}(\rho) \\ C_2(\rho) & D_{21}(\rho) & D_{22}(\rho) \end{bmatrix} \begin{bmatrix} x(t) \\ d(t) \\ u(t) \end{bmatrix}, \tag{3}$$

where $\rho \in \mathcal{F}_\mathcal{P}$, $y \in \mathcal{R}^{n_y}$ is the measurement, $u \in \mathcal{R}^{n_u}$ is the control input, $d \in \mathcal{R}^{n_d}$ is the exogenous disturbance, and $e \in \mathcal{R}^{n_e}$ is the error output. It is assumed that the parameter $\rho(\cdot)$ can be measured in real-time, and that the controller is of the form

$$\begin{bmatrix} \dot{x}_K(t) \\ u(t) \end{bmatrix} = \begin{bmatrix} A_K(\rho(t)) & B_K(\rho(t)) \\ C_K(\rho(t)) & D_K(\rho(t)) \end{bmatrix} \begin{bmatrix} x_K(t) \\ y(t) \end{bmatrix}, \tag{4}$$

where $\rho \in \mathcal{F}_{\mathcal{P}}$.

The "quadratic LPV γ-performance problem" is to choose the parameter-varying controller matrices $A_K(\rho),\ B_K(\rho),\ C_K(\rho),\ D_K(\rho)$ such that the resultant closed-loop system is quadratically stable and the induced $\mathcal{L}_2$ norm from d to e is $\leq \gamma$. It is well known that the quadratic LPV γ-performance problem is solvable if there exists an integer $m \geq 0$, a matrix $W \in \mathcal{R}^{(n+m)\times(m+n)}$, $W = W^T > 0$ and continuous bounded matrix functions $(A_K, B_K, C_K, D_K) : \mathcal{R}^s \to (\mathcal{R}^{m\times m}, \mathcal{R}^{m\times n_y}, \mathcal{R}^{n_u\times m}, \mathcal{R}^{n_u\times n_y})$ such that

$$\begin{bmatrix} A_{clp}^T(\rho)W + WA_{clp}^T(\rho) & WB_{clp}(\rho) & \gamma^{-1}C_{clp}^T(\rho) \\ B_{clp}^T(\rho)W & -I_{n_d} & \gamma^{-1}D_{clp}^T(\rho) \\ \gamma^{-1}C_{clp}(\rho) & \gamma^{-1}D_{clp}(\rho) & -I_{n_e} \end{bmatrix} < 0, \tag{5}$$

for all $\rho \in \mathcal{P}$, where the matrices A_{clp}, B_{clp}, C_{clp} and D_{clp} are the closed-loop state-space data.

The main result is that the existence of a controller that solves the quadratic LPV γ-performance problem can be expressed as the feasibility of a set of Affine Matrix Inequalities (AMIs), which can be solved numerically. For more details on LPV synthesis results the reader is referred to [13, 14]. The parameter ρ is assumed to be available in real time, and hence it is possible to construct an LPV controller whose dynamics adjust according to variations in ρ, and maintain stability and performance along all parameter trajectories. This approach allows gain-scheduled controllers to be treated as a single entity, with the gain-scheduling achieved via the parameter-dependent controller.

The goal of this paper is to design nonlinear suspension controllers that emphasize a different performance objective, depending on the magnitude of suspension deflection. When the suspension deflection is small the controller should focus on passenger comfort. As the deflection limit is approached the controller should focus on preventing the suspension deflection from exceeding this limit. Hence, in our case the scheduling variable ρ is the suspension deflection. Even though the parameter ρ, i.e., suspension deflection, is generated by the vehicle dynamics we assume that it is an exogenous time-varying parameter during the design stage. The LPV controller (4) is implemented by setting the parameter ρ to be equal to the suspension deflection. It is important to note that since the LPV controller guarantees stability and performance over the whole parameter variation set $\mathcal{F}_{\mathcal{P}}$, i.e., even over infinitely fast variations of $\rho(\cdot)$ between values in $\mathcal{P}$, setting ρ to be equal to the suspension deflection during implementation does not compromise stability and performance.

In this paper we model the suspension assembly as a linear time-invariant system, composed of masses, springs and dampers (see Figure 1 below). As is common in standard $\mathcal{H}_\infty$ design, we augment the suspension model with weighting functions in order to capture the performance objectives. The difference here is that in order to capture the shift in focus from comfort to suspension deflection, these weighting functions are chosen to be dependent on the parameter ρ. This results in a control design interconnection that is linear parameter-varying in nature (see Figure 2). The LPV controller (4) is designed using the plant data, i.e., (3), that corresponds to this interconnection.

3 Quarter car suspension model and fundamental performance tradeoffs

The quarter car model shown in Figure 1 will be used to design active suspension control laws. This model has been used extensively in the literature and captures many important characteristics of more detailed models. In Figure 1 the sprung mass, m_s, represents the car chassis, while the unsprung mass, m_{us}, represents the wheel assembly. The spring, k_s, and damper, b_s, represent a passive spring and shock absorber that are placed between the car body and the wheel assembly, while the spring, k_t, serves to model the compressibility of the pneumatic tyre. The variables x_s, x_{us}, and r are the car body travel, the wheel travel, and the road disturbance respectively. The force f_s applied between the sprung and unsprung masses, is controlled by feedback and represents the active component of the suspension system. This force is generated by means of a hydraulic actuator placed between the two masses (see [7, 8] for details). As is common in the literature, we shall ignore the dynamics of the actuator, and assume that the control signal is the force f_s. We assume that x_s and x_{us} are measured from their static equilibrium positions and that the tyre remains in contact with the road at all times. Defining $x_1 := x_s$, $x_2 := \dot{x_s}$,

$x_3 := x_{us}$ and $x_4 := \dot{x}_{us}$, we have the following state-space description of the quarter car dynamics.

$$\begin{aligned}
\dot{x_1} &= x_2, \\
\dot{x_2} &= -\frac{1}{m_s}[k_s(x_1 - x_3) + b_s(x_2 - x_4) - f_s], \\
\dot{x_3} &= x_4, \\
\dot{x_4} &= \frac{1}{m_{us}}[k_s(x_1 - x_3) + b_s(x_2 - x_4) - k_t(x_3 - r) - f_s]. \qquad (6)
\end{aligned}$$

The following component values are taken from reference [8].

$$\begin{aligned}
m_s &= 290 \text{ kg}\ , \\
m_{us} &= 59 \text{ kg}\ , \\
b_s &= 1000 \text{ N/m/s}\ , \\
k_s &= 16812 \text{ N/m}\ , \\
k_t &= 190000 \text{ N/m}\ . \qquad (7)
\end{aligned}$$

3.1 Tradeoffs between passenger comfort and suspension deflection

The three main performance metrics in suspension design are passenger comfort, suspension deflection and road holding ability. In this paper we shall focus on the first two. It is widely accepted that there is a good correlation between the degree of passenger comfort and the vertical acceleration experienced by the car body. In order to improve passenger comfort it is important to keep the transfer function $H_a(s)$ from the road disturbance r to the car body acceleration $\ddot{x}_1$ small in the 0-65 rad/sec frequency range. Structural features of the vehicle place a hard limit on the amount of suspension deflection $x_1 - x_3$ available to reduce the vertical acceleration of the car body. Hitting the deflection limit results in not only considerable passenger discomfort, but increases the wear of the vehicle. In this paper we shall assume that the suspension travel is limited to 8 cm. Hence it is also important to keep the transfer function $H_{sd}(s)$ from the road disturbance r to the suspension deflection $x_1 - x_3$ small enough to prevent the deflection limit from being reached.

It is well known [15] that the acceleration transfer function $H_a(s) := \frac{\ddot{X}_1(s)}{R(s)}$ has an invariant point at the *tyrehop frequency*, $\omega_1 = \sqrt{k_t/m_{us}}$, i.e., the transfer function at this frequency depends only on k_t, m_u and m_{us}. From the point of view of control design this means that the transfer function from f_s to $\ddot{x}_1$ has a zero at ω_1. For the parameter values listed in equation (7), $\omega_1 = 56.7$ rad/sec. Similarly, the suspension deflection transfer function $H_{sd}(s) := \frac{X_1(s)-X_3(s)}{R(s)}$ has an invariant point at the *rattlespace frequency*, $\omega_2 = \sqrt{k_t/(m_{us}+m_s)}$. Once again this means that the transfer function from f_s to $x_1 - x_3$ has a zero at ω_2. In our case $\omega_2 = 23.3$ rad/sec. The tradeoff between passenger comfort and suspension deflection is due to the fact that is is not possible to simultaneously keep both the above transfer functions small around the tyrehop frequency and in the low frequency range. In [15] it is shown that a small reduction in vertical acceleration at low frequencies and in the vicinity of the tyrehop frequency results in a large increase in suspension deflection at these frequencies and vice versa. Suspension controllers designed using linear methods represent a tradeoff between these conflicting tendencies.

The need for the above compromise is really an artifact of the control design method, namely linear control. Suspension deflection is a hard constraint and hence ideally the active controller should focus on it only when it is close to the allowable limit. Under normal road conditions i.e., when suspension travel is small, the controller should focus on keeping the vertical acceleration as small as possible without regard for the deflection constraint. Such a controller switches from minimizing the acceleration “frequency response” to keeping the deflection “frequency response” small, depending on the suspension travel. This change in focus is a property that a linear controller can never achieve. Only nonlinear controllers can achieve this objective and hence have the potential of providing superior ride quality throughout the range of road surfaces, when compared to linear controllers.

4 Linear $\mathcal{H}_\infty$ controller design

In this section we discuss the design of linear suspension controllers that emphasize either passenger comfort or suspension deflection. As discussed above, a controller that focuses on passenger comfort, i.e., keeps the acceleration transfer function small, does so at the expense of large suspension deflection, and vice versa. The goal of this section is to establish a baseline for the amount of reduction in vertical acceleration and suspension deflection that can be achieved, when these metrics are minimized independently. In later sections these designs will be combined into a single nonlinear controller that emphasizes acceleration when suspension deflection is small, and suspension deflection when the deflection is close to its structural limit. The controllers in this section are designed using linear $\mathcal{H}_\infty$ synthesis. As is standard in the $\mathcal{H}_\infty$ framework, the performance objectives are achieved via minimizing weighted transfer function norms. Weighting functions serve two purposes in the $\mathcal{H}_\infty$ framework: they allow the direct comparison of different performance objectives with the same norm and they allow for frequency information to be incorporated into the analysis. For more details on $\mathcal{H}_\infty$ control design the reader is referred to [16, 17] and the references therein. A block diagram of the $\mathcal{H}_\infty$ control design interconnection is shown in Figure 2.

The measured output or feedback signal, y, is the suspension deflection $x_1 - x_3$. The controller acts on this signal to produce the control input to the suspension model, namely the hydraulic actuator force f_s. Typically the block W_n serves to model sensor noise in the measurement channel. We set $W_n = 10^{-5}$, thus essentially ignoring the sensor noise. However by assuming that W_n is small but non zero, we ensure that certain rank conditions (see [17]) associated with $\mathcal{H}_\infty$ synthesis are satisfied. In a more realistic design W_n would be frequency dependent, and would serve to model the noise associated with the displacement sensor. The weight W_{ref} is used to scale the magnitude of the road disturbances. We assume that the maximum road disturbance is 11 cm and hence choose $W_{ref} = 0.11$.

The magnitude and frequency content of the control force f_s is limited by the weighting function W_{act}. We choose $W_{act} = \frac{0.5/1300(s+50)}{s+500}$. The magnitude of the weight increases above 50 rad/sec in order to limit the closed-loop bandwidth. The purpose of the weighting functions W_{x_1} and $W_{x_1-x_3}$ is to keep the acceleration and the suspension deflection small over the desired frequency ranges. Observe that instead of penalizing vertical acceleration, i.e., $\ddot{x}_1$, we are penalizing the body travel x_1. The $\mathcal{H}_\infty$ designs of the present section are easily redone with an appropriate weight on the acceleration ($\ddot{x}_1$) signal instead of body travel (x_1). However, it was our experience that penalizing x_1 resulted in less conservative LPV designs, than those that resulted from penalizing $\ddot{x}_1$. We choose

$$W_{x_1}(s) = \frac{\phi_a \cdot 2\pi 5}{s + 2\pi 5},$$

and

$$W_{x_1 - x_3}(s) = \frac{\phi_d \cdot 10}{s + 10},$$

where ϕ_a and ϕ_d are gains that reflect the relative importance we place on the acceleration and deflection transfer functions in the $\mathcal{H}_\infty$ design. A large gain ϕ_a and a small gain ϕ_d corresponds to a design that emphasizes passenger comfort. On the other hand, choosing ϕ_a small and ϕ_d large corresponds to a design that focuses on suspension deflection. We now discuss control designs that are based on the above two choices of ϕ_a and ϕ_d.

Design 1: In this design we focus on keeping the acceleration transfer function small, without regard for the suspension deflection transfer function. Therefore we choose $\phi_a = 25$ and set $\phi_d = 0$. A magnitude plot of the weight $W_{x_1}(s)$ is shown by the dashed line in Figure 3, from which it is seen that the magnitude rolls off above $2\pi 5$ rad/sec. The $2\pi 5$ rad/sec rolloff was chosen to respect the well-known $\mathcal{H}_\infty$ design rule-of-thumb that requires the performance weights to roll off before an open-loop zero (56.7 rad/sec in this case). We do not roll the weight back up after the zero since we are only interested in acceleration performance in the 0-65 rad/sec frequency range. In any case, as shown in reference [18], $H_a(s) = O(s^{-2})$ (i.e., $s^2 H_a(s)$ tends to a finite, possibly zero, limit as $s \to \infty$), and hence penalizing acceleration at higher frequencies offers no significant benefit.

The dashed lines in Figure 4 are the closed-loop frequency responses that result from this choice of weighting functions. For comparison purposes the frequency responses of the passive suspension, i.e., $f_s = 0$, are also displayed by the solid line. Observe the reduction in acceleration in the low frequency range, and the corresponding increase in suspension deflection in this range. The acceleration response is close to the passive response in the vicinity of the tyrehop frequency $\omega_1 = 56.7$ rad/sec. This is due to the fact the tyrehop frequency is an invariant point and hence the magnitude of the response at this point cannot be altered by feedback. $\square$

Design 2: In this design we focus on keeping the suspension deflection transfer function small, without regard for the acceleration transfer function. Therefore we choose $\phi_d = 200$ and set $\phi_a = 0$. A magnitude plot of the weight $W_{x_1-x_3}(s)$ is shown by the dotted line in Figure 3, from which it is seen that the magnitude rolls off above 10 rad/sec. The 10 rad/sec rolloff was chosen to respect the well-known $\mathcal{H}_\infty$ design rule-of-thumb that requires the performance weights to roll off before an open-loop zero (23.3 rad/sec in this case). We do not roll the weight back up after the zero since, as shown in [18], $H_{sd}(s) = -\frac{k_t}{m_{us}}s^{-2} + O(s^{-4})$ (see [18]) and as a consequence the high frequency asymptote of $H_{sd}(s)$ is independent of the control law.

The dotted lines in Figure 4 are the closed-loop frequency responses that result from this choice of weighting functions. Observe the reduction in suspension deflection in the vicinity of the tyrehop frequency $\omega_1 = 56.7$ rad/sec, and the corresponding increase in the acceleration frequency response in this vicinity. Also, compared to Design 1, a reduction in suspension deflection has been achieved for frequencies below the rattlespace frequency $\omega_2 = 23.3$ rad/sec. $\square$

The time responses of these two controllers are shown in Figures 5 and 6. The dash-dot, dashed and dotted lines correspond to the passive suspension, Design 1 and Design 2 respectively. All responses correspond to the road disturbance $r(t)$ used in [8]:

$$\begin{aligned} r(t) &= a(1-\cos 8\pi t), \quad 0.5 \le t \le 0.75, \\ &= 0 \quad \text{otherwise}\ , \end{aligned} \tag{8}$$

where $a = 0.025$ and $a = 0.055$ correspond to road bumps of peak magnitude 5 cm and 11 cm respectively. Figure 5 shows the suspension response for $a = 0.025$, i.e., a 5 cm bump, whereas Figure 6 corresponds to $a = 0.055$, i.e., a 11 cm bump. Observe that the acceleration response of Design 1 to the 5 cm bump is very good (see Figure 5). However the suspension deflection in response to the 11 cm bump hits the 8 cm limit, resulting in a large vertical acceleration being transmitted to the car body (see Figure 6). This is due to the fact that suspension deflection was not penalized in this design. The suspension deflection response of Design 2 to a 11 cm bump is well within the allowable limit (see Figure 6). However the acceleration response to the 5 cm bump is much inferior to Design 1 (see Figure 5). Once again this is due to the fact that acceleration was not penalized in Design 2.

Remark 1: In the above simulations the suspension deflection was prevented from exceeding its limit by a sharp increase in the spring and damper constants, k_s and b_s, as the deflection limit is reached. The resulting acceleration that is transmitted to the car body (600 to 800 m/s^2) is of the same order of magnitude as that shown in reference [8, Figure 11], and hence may be considered representative of the amount of acceleration transmitted to the car body when the deflection limits are hit. In order to clearly display the acceleration magnitudes for those responses that do not violate the suspension limit, the acceleration axis was limited to 100 m/s^2 and hence the higher accelerations are not apparent in the plots.

Designs 1 and 2 represent extreme ends of the performance tradeoff spectrum. Conventional linear suspension controllers lie between these two extremes and seek to establish a tradeoff between acceleration and suspension deflection response characteristics. In the next section we shall combine the above linear controllers into a single nonlinear controller using linear parameter-varying control design.

5 Nonlinear Controller Design

In this section the two linear $\mathcal{H}_\infty$ controllers designed above are combined into a single linear parameter-varying (LPV) controller. The LPV controller schedules on suspension deflection, i.e., $\rho = x_1 - x_3$, and focuses on minimizing either the vertical acceleration or suspension deflection response, depending on the magnitude of the suspension deflection. The control design interconnection used for synthesizing the LPV controller is the same as that shown in Figure 2, with the difference that some of the weighting functions are now dependent on the parameter ρ.

The weights W_{ref} and W_n are the same as those used in the $\mathcal{H}_\infty$ point designs. Since LPV controllers typically tend to have higher bandwidths than their $\mathcal{H}_\infty$ point design counterparts, the actuator weighting function gain was doubled in the LPV design. In order to achieve the shift in focus from vertical acceleration to suspension deflection the weights associated with these signals, i.e., W_{x_1} and $W_{x_1-x_3}$, are chosen to be parameter-dependent, i.e., functions of ρ. We choose $W_{x_1}[\rho]$ to have a realization,

$$\begin{aligned} \dot{x} &= -2\pi 5x + \sqrt{2\pi 5\phi_a[\rho]}\ u, \\ y &= \sqrt{2\pi 5\phi_a[\rho]}\ x, \end{aligned}$$

and $W_{x_1-x_3}[\rho]$ to have a realization,

$$\begin{aligned} \dot{x} &= -10x + \sqrt{10\phi_d[\rho]}\ u, \\ y &= \sqrt{10\phi_d[\rho]}\ x, \end{aligned}$$

where the parameter-dependent gains $\phi_a[\rho]$ and $\phi_d[\rho]$ capture the relative importance of the acceleration and deflection responses, as a function of suspension deflection. When ρ is small, i.e., when the suspension deflection is well away from its limits, $\phi_a[\rho]$ is large and $\phi_d[\rho]$ is small, indicating that the LPV controller should focus on minimizing acceleration without regard for suspension deflection. On the other hand, when ρ approaches the 8 cm limit $\phi_d[\rho]$ is large and $\phi_a[\rho]$ is small, indicating that the controller should focus on preventing the deflection limit from being reached. In this paper the parameter dependence of the gains $\phi_a[\rho]$ and $\phi_d[\rho]$ is characterized by means of two constants ρ_1 and ρ_2, where $\rho_2 > \rho_1 \geq 0$. The constant ρ_1 defines the magnitude of suspension travel at which the suspension starts to stiffen, whereas ρ_2 determines how fast this stiffening occurs. Based on this we define

$$\begin{aligned} \phi_a[\rho] &= 25 \quad \text{if} \quad |\rho| < \rho_1, \\ &= \frac{25}{\rho_1 - \rho_2}[|\rho| - \rho_2] \text{ if } \rho_1 \leq |\rho| \leq \rho_2, \\ &= 0 \quad \text{otherwise} \ , \end{aligned}$$

and the gain $\phi_d[\rho]$ as

$$\begin{aligned} \phi_d[\rho] &= 0 \quad \text{if} \quad |\rho| < \rho_1, \\ &= \frac{200}{\rho_2 - \rho_1}[|\rho| - \rho_1] \text{ if } \rho_1 \leq |\rho| \leq \rho_2, \\ &= 200 \quad \text{otherwise} \ . \end{aligned}$$

It is clear from the above definitions that a small ρ_1 and large ρ_2 corresponds to a suspension that stiffens early and gradually, whereas a large ρ_1 and small $\rho_2 - \rho_1$ corresponds to a suspension that stiffens very rapidly when the deflection is close to the allowable limit. For our design we choose $\rho_1 = 0.0575$ and $\rho_2 = 0.08$. This choice corresponds to a LPV controller that minimizes only the vertical acceleration when the suspension travel is less than 5.75 cm, and gradually begins focusing on the suspension deflection when the travel is greater than 5.75 cm. A plot of $\phi_a[\rho]$ and $\phi_d[\rho]$ for this choice of ρ_1/ρ_2 is shown in Figure 7.

Remark 2: The state-space realization of the weights $W_{x_1}[\rho]$ and $W_{x_1-x_3}[\rho]$ are of great importance. For example, an alternative realization of $W_{x_1}[\rho]$ could be

$$\begin{aligned} \dot{x} &= -2\pi 5x + 2\pi 5\phi_a[\rho]\ u, \\ y &= x. \end{aligned}$$

Although both realizations have identical input-output behavior for constant ρ, this is not true when $\rho(t)$ is non-constant. In the second realization the output is always a continuous function of time, whereas in the first realization this is not the case. Hence, from a parameter-varying perspective, these realizations result in different control design interconnections. Our goal is to design the LPV controller such that the closed-loop frequency response with the controller 'frozen' at the two extreme parameter values, i.e., $\rho = 0$ and 0.08 is close to the response of the linear $\mathcal{H}_\infty$ control Designs 1 and 2. Experimentation with a variety of realizations showed that the chosen realizations best achieve this objective.

5.1 LPV Controller Synthesis

The synthesis of an LPV controller for the control design interconnection of Figure 2 involves solving a set of affine matrix inequalities (AMI's) (see [13] for details). The AMI's represent an infinite number of constraints since the inequalities must hold for each parameter value. For computational purposes, these are approximated by a finite number of constraints by gridding of the parameter space. As a consequence, the LPV controller that results is defined only at the grid points. Typically, linear interpolation between these controller points is employed in order to define the controller as a continuous function of the parameter values. In the present design we choose only two grid points: $\rho_1 = 0.0575$ and $\rho_2 = 0.08$. It follows from our choice of parameter-dependent weights (see Figure 7), that these grid points capture the control design interconnection of Figure 2 for all parameter values that lie in the intervals $[-\rho_1, \rho_1]$, $(-\infty, -\rho_2]$, and $[\rho_2, \infty)$. Adding additional grid points in the remaining intervals, $[-\rho_2, -\rho_1]$ and $[\rho_1, \rho_2]$, offers little benefit since the value of the gains, $\phi_a[\rho]$ and $\phi_d[\rho]$, in these intervals is simply a linear interpolation of the values at the endpoints.

Since we have only two grid points, solving the two sets of associated AMI's results in an LPV controller that is defined at only these parameter values, i.e., $K[\rho_1] := (A_1, B_1, C_1, D_1)$ and $K[\rho_2] := (A_2, B_2, C_2, D_2)$. The LPV controller is implemented by linearly interpolating between these two controller points as follows:

$$\begin{aligned} K[\rho] &:= (A_1, B_1, C_1, D_1), \text{ if } \rho \in [-\rho_1, \rho_1], \\ &:= (A_2, B_2, C_2, D_2), \text{ if } \rho \in (-\infty, -\rho_2] \text{ or } [\rho_2, \infty) \\ &:= (A(\rho), B(\rho), C(\rho), D(\rho)), \text{ if } \rho \in (\rho_1, \rho_2), \\ &:= (A(-\rho), B(-\rho), C(-\rho), D(-\rho)), \text{ if } \rho \in (-\rho_2, -\rho_1), \end{aligned} \tag{9}$$

where $A(\rho) := \frac{A_1 - A_2}{\rho_1 - \rho_2}(\rho - \rho_1) + A_1$, $B(\rho) := \frac{B_1 - B_2}{\rho_1 - \rho_2}(\rho - \rho_1) + B_1$, $C(\rho) := \frac{C_1 - C_2}{\rho_1 - \rho_2}(\rho - \rho_1) + C_1$, and $D(\rho) := \frac{D_1 - D_2}{\rho_1 - \rho_2}(\rho - \rho_1) + D_1$.

Remark 3: Due to the parameter space gridding necessary to numerically solve for the LPV controller, closed-loop stability is no longer guaranteed over all parameter trajectories, as would be the case if the infinite set of AMIs were solved analytically. Hence, simulation of the resulting closed-loop system is necessary to check the stability/performance of the implemented closed-loop system. Experience has shown that if the gridding is fine enough stability/performance with the implemented LPV controller is generally not an issue.

Implementation of the LPV controller requires storing the values of the controller at each grid point and interpoling between these points during closed-loop operation. Since, in general, the LPV controller has different values at different grid points, too fine a parameter grid can result in designs that may be prohibitive from the point of view of storage. Since our LPV controller has only two unique defining values we believe that it should be easy to implement in practice.

5.2 LPV controller analysis

In Figure 8 we show the closed-loop frequency response plots with the LPV controller frozen at $\rho = 0$ (dashed) and $\rho = 0.08$ (dotted). These parameter values correspond to a focus on comfort and suspension travel respectively, as can be seen from the plots in the figure. The solid line is the frequency response of the passive suspension.

The time responses of the LPV controller are shown in Figures 5 and 6. In the simulations, the LPV controller is implemented by setting the scheduling variable, ρ, to be equal to the suspension deflection, i.e., $\rho(t) = x_1(t) - x_3(t)$. The solid, dashed and dotted lines correspond to the LPV design, $\mathcal{H}_\infty$ Design 1 and $\mathcal{H}_\infty$ Design 2 respectively. Once again all responses correspond to the road disturbance defined as in equation (8). Figures 5 and 6 correspond to $a = 0.025$ (5 cm bump) and $a = 0.055$ (11 cm bump) respectively . Observe that the acceleration response of the LPV controller to the 5 cm bump is close to that of Design 1 (see Figure 5). The reason for this is that we set $\rho_1 = 0.0575$, and hence the LPV controller focuses on minimizing only vertical acceleration for bumps of height less than approximately 5 cm. The response of the LPV controller to the 11 cm bump is initially close to that of Design 1 (see Figure 6). As the suspension deflection limit of 8 cm is approached the controller schedules between $K[\rho_1]$ and $K[\rho_2]$ to prevent this limit from being reached. Since $\rho_1 = 0.0575$, the LPV controller begins to limit suspension travel when this travel exceeds 5.75 cm. Hence, the vertical acceleration transmitted to the car body in the process of preventing the limit from being reached is much smaller than that transmitted if the limit were hit (see for example the response of Design 1 to the 11 cm bump in Figure 6).

We now study the effect of varying the design parameter ρ_1 on the nonlinear response of the suspension. Recall that for a fixed value of the parameter ρ_2, the parameter ρ_1 determines at what point and how fast the suspension starts to stiffen. Small values of ρ_1 correspond to suspensions that stiffen early and gradually, whereas large values of ρ_1 correspond to suspensions that stiffen rapidly when the travel is close to the limit. In Figure 9 we plot the peak suspension deflection magnitude against road bump height for bumps as described in equation (8). We keep ρ_2 fixed at 0.08 and vary ρ_1. The dash-dot, solid and dashed lines correspond to $\rho_1 = 0,\ 0.0575,$ and 0.07 respectively. With $\rho_1 = 0$ the suspension exhibits a gradual stiffening, whereas when $\rho_1 = 0.07$ the response is linear for the bumps of height upto about 7 cm, and stiffens rapidly thereafter. Thus the design parameters ρ_1 and ρ_2 can be used to shape the nonlinear response characteristics of the suspension.

6 Road adaptive suspension design

In the preceding sections we have used linear parameter-varying gain-scheduling techniques to design a nonlinear control law that focuses on either passenger comfort or suspension deflection, depending on how close the suspension deflection is to its maximum limits. This was accomplished by using weighting functions whose gains depend on the scheduling variable, i.e., suspension deflection. In the more general case a third performance metric needs to be considered, namely road holding. Good road holding performance translates into small tyre deflection, $x_3 - r$. The importance of road holding performance depends on the driving condition, e.g., road holding is important during sharp turns and may be relaxed on straight road sections.

In order to incorporate road holding in the present framework, the lateral acceleration, a_{lat}, can be introduced as a second gain-scheduling parameter. An additional weighting function W_{x_3-r} can be included on the signal $x_3 - r$, and all the three weighting functions will have a two-dimensional parameter-dependence, i.e., $W_{x_1}[x_1 - x_3, a_{lat}]$, $W_{x_1-x_3}[x_1 - x_3, a_{lat}]$, and $W_{x_3-r}[x_1 - x_3, a_{lat}]$. The weight $W_{x_3-r}[x_1 - x_3, a_{lat}]$ is large when a_{lat} is large, i.e., during sharp cornering, and is small when a_{lat} is close to zero, i.e., during straight road sections. The nonlinear controller in this case will depend on $x_1 - x_3$ and a_{lat}, i.e., $K[x_1 - x_3, a_{lat}]$.

Another possible extension of the framework proposed here is to the design of road adaptive vehicle suspensions. At the end of the previous section we showed how the design parameters ρ_1 and ρ_2 can be used to shape the nonlinear response characteristics of the suspension (see Figure 9). If the road is essentially smooth (except for the occasional large pothole, eg., a highway), it would be preferable to choose ρ_1 large and $\rho_2 - \rho_1$ small, e.g., the dashed line in Figure 9. This corresponds to a suspension that is linear for the most part, and stiffens very rapidly as the suspension limits are reached. Although this would result in a large vertical acceleration as the limit is being reached (yet much smaller than that transmitted if the limit were hit) this would be a small price to pay for the superior comfort over the smooth sections. On the other hand, if the road section is essentially rough it would be preferable to choose ρ_1 close to zero and ρ_2 large, e.g., the dash-dot line in Figure 9. This corresponds to a suspension that gradually stiffens over the range of operation. Over rough roads this choice would result in smaller vertical accelerations than those corresponding to the previous choice. Thus, the design parameters ρ_1 and ρ_2 can be chosen to be parameter-dependent as well. The additional scheduling parameter in this case could be the average suspension deflection over a fixed time window. This average can be computed on-line and based on it the LPV controller schedules so as to correspond to the appropriate ρ_1/ρ_2 setting. This adaptive feature would lead to superior passenger comfort over the whole range of road conditions.

7 Conclusions

In this paper we have proposed a framework for the design of nonlinear active suspensions. Using linear parameter-varying control techniques we have designed controllers that focus on either passenger comfort or suspension deflection, depending on the magnitude of suspension deflection. Simulations show that the present controller provides superior performance as compared to fixed linear controllers. Conceptually, the framework extends to handle more general design problems such as road adaptive suspension design. These extensions are the focus of ongoing investigation.

References

[1] Roley, D.G., "Tractor cab suspension modeling", *Ph.D Thesis*, University of California, Davis, 1975.

[2] Metz, D. and Maddock, J., "Optimal ride height and pitch control for championship race cars", *Automatica*, 22 (1986), pp. 509-520.

[3] Hrovat, D., "Optimal Active Suspension Structures for Quarter-car Vehicle Models", *Automatica*, 26 (1990), pp. 845-860.

[4] Hrovat, D., "Applications of Optimal Control to Advanced Automotive Suspension Design", *Transactions of the ASME, Journal of Dynamic Systems, Measurement, and Control*, 115 (1993), pp. 328-342.

[5] Thompson, A.G., "An Active Suspension with Optimal Linear State Feedback", *Vehicle System Dynamics*, 5 (1976), pp. 187-203.

[6] Thompson, A.G., "Optimal and Suboptimal Linear Active Suspensions for Road Vehicles", *Vehicle System Dynamics*, 13 (1984), pp. 61-72.

[7] Alleyne, A., Neuhaus, P.D. and Hedrick, J.K., "Application of Nonlinear Control Theory to Electronically Controlled Suspensions", *Vehicle System Dynamics*, 22 (1993), pp. 309-320.

[8] Lin, J. and Kanellakopoulos, I., "Nonlinear Design of Active Suspensions", *Control Systems*, 17 (1997), pp. 45-59.

[9] Sunwoo, M. and Cheok, K.C., "An Application of Explicit Self-Tuning Controller to Vehicle Active Suspension Systems", *Proceedings of the IEEE Conference on Decision and Control* (1990), pp. 2251-2255.

[10] Chalasani, R.M., "Ride performance potential of active suspension systems - Part 1, *ASME Monograph*, AMD Vol. 80, DSC, Vol 2, 1986.

[11] Kristic, M., Kanellakopoulos, I. and Kokotovic, P., "Nonlinear and Adaptive Control Design", *Wiley Inter-Science*, 1995.

[12] Lin, J. and Kanellakopoulos, I., "Road Adaptive Nonlinear Design of Active Suspensions", *Proceedings of the American Control Conference* (1997), pp. 714-718.

[13] Becker, G., "Quadratic Stability and Performance of Linear Parameter Dependent Systems", *Ph.D. Thesis*, Department of Mechanical Engineering, University of California at Berkeley, 1993.

[14] Becker, G. and Packard, A., “Robust Performance of Linear Parametrically Varying Systems Using Parametrically Dependent Linear Dynamic Feedback” *System and Control Letters*, 23 (1994), pp. 205-215.

[15] Hedrick, J.K. and Batsuen, T., “Invariant Properties of Automotive Suspensions”, *Proceedings of The Institution of Mechanical Engineers*, 204 (1990), pp. 21-27.

[16] Balas, G. and Doyle, J., “Robustness and performance tradeoffs in control design for flexible structures”, *IEEE Transactions on Control Systems Technology*, vol. 2, no. 4 (1994), pp. 352-361.

[17] Balas, G., Doyle, J., Glover, K., Packard, A. and Smith, R., “The μ Analysis and Synthesis Toolbox”, *MUSYN and The Mathworks*, 1993.

[18] Smith, M.C., “Achievable Dynamic Response for Automotive Active Suspensions”, *Vehicle System Dynamics*, vol. 24 (1995), pp. 1-34.

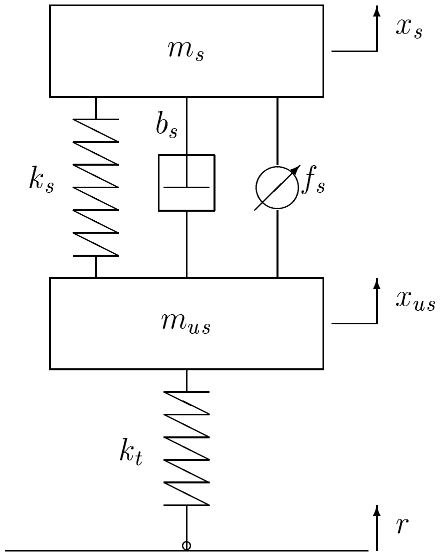

Figure 1: Quarter Car Model

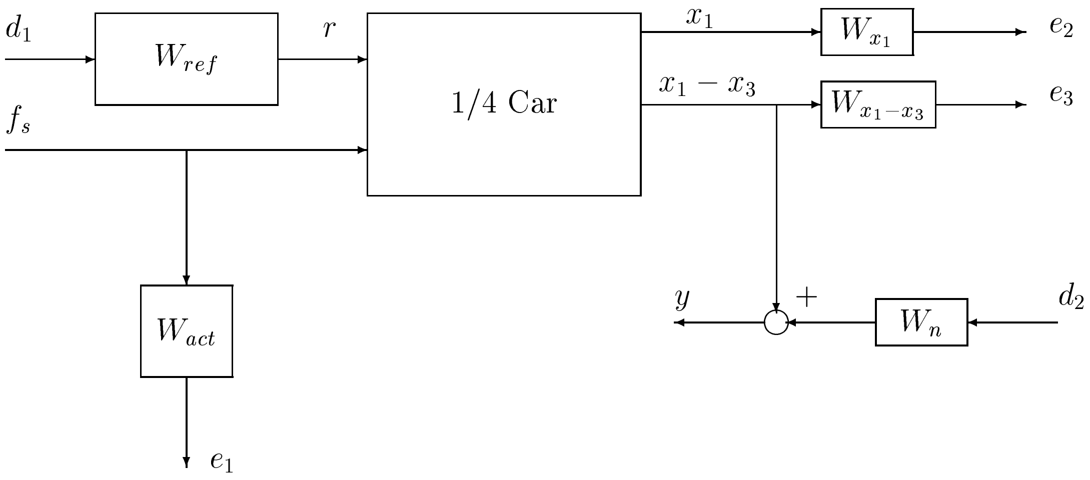

Figure 2: $\mathcal{H}_\infty$ control design interconnection

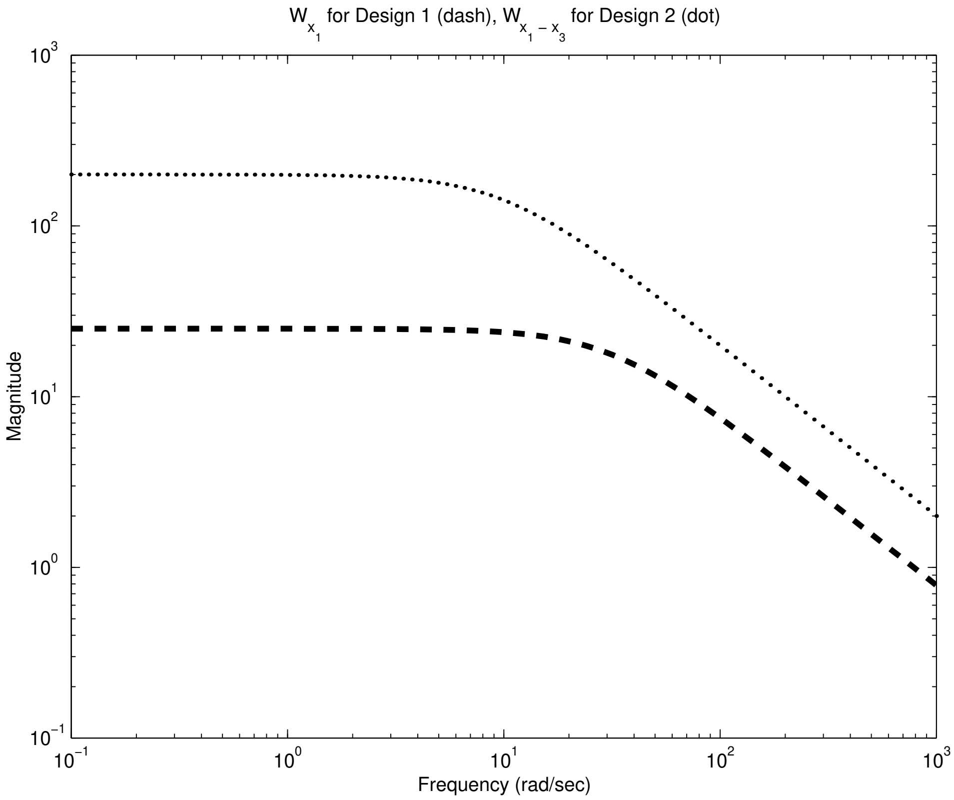

Figure 3: $W_{x_1}(s)$ for Design 1: $\phi_a = 25$ (dash), $W_{x_1 - x_3}(s)$ for Design 2: $\phi_d = 200$ (dot)

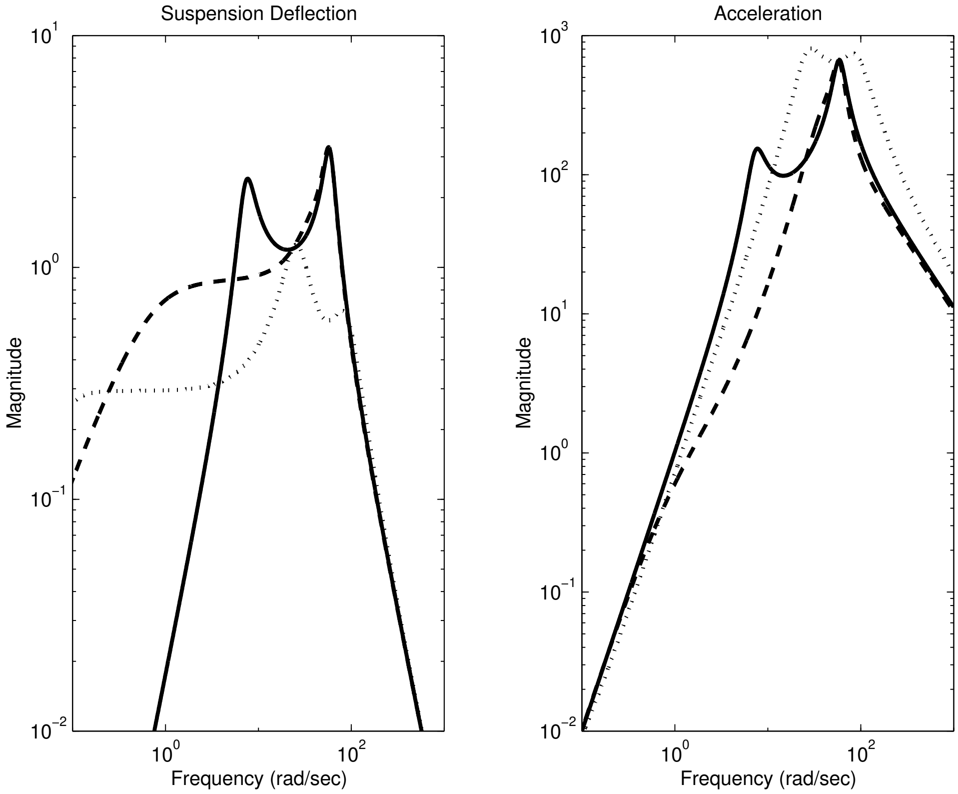

Figure 4: $\mathcal{H}_\infty$ controller: closed-loop frequency responses, Design 1 (dash), Design 2 (dot), Passive (solid)

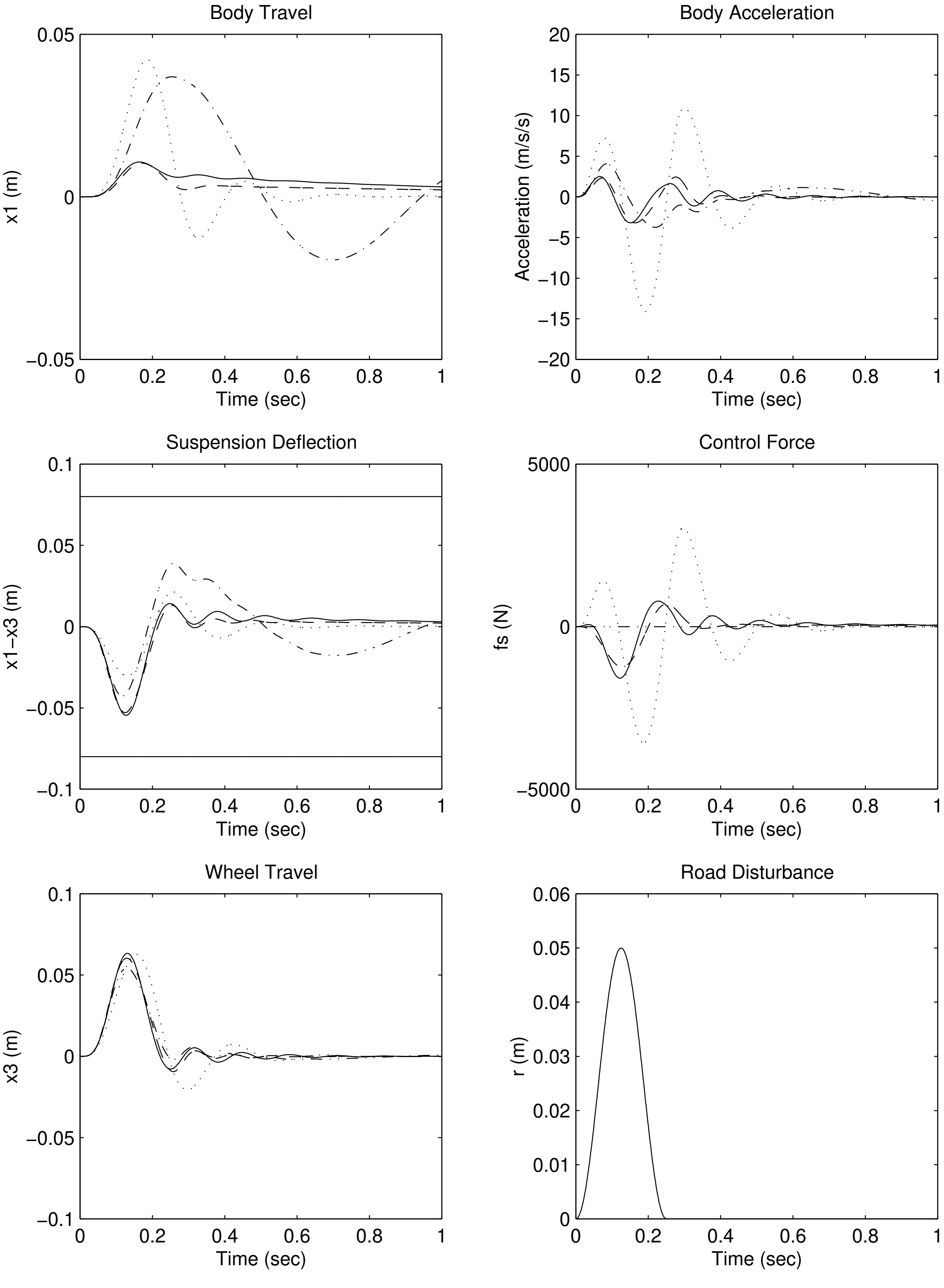

Figure 5: $\mathcal{H}_\infty$ controller responses to a 5 cm bump, Passive (dash-dot), Design 1 (dash), Design 2 (dot), LPV (solid). The solid horizontal lines in the suspension deflection window are the deflection limits.

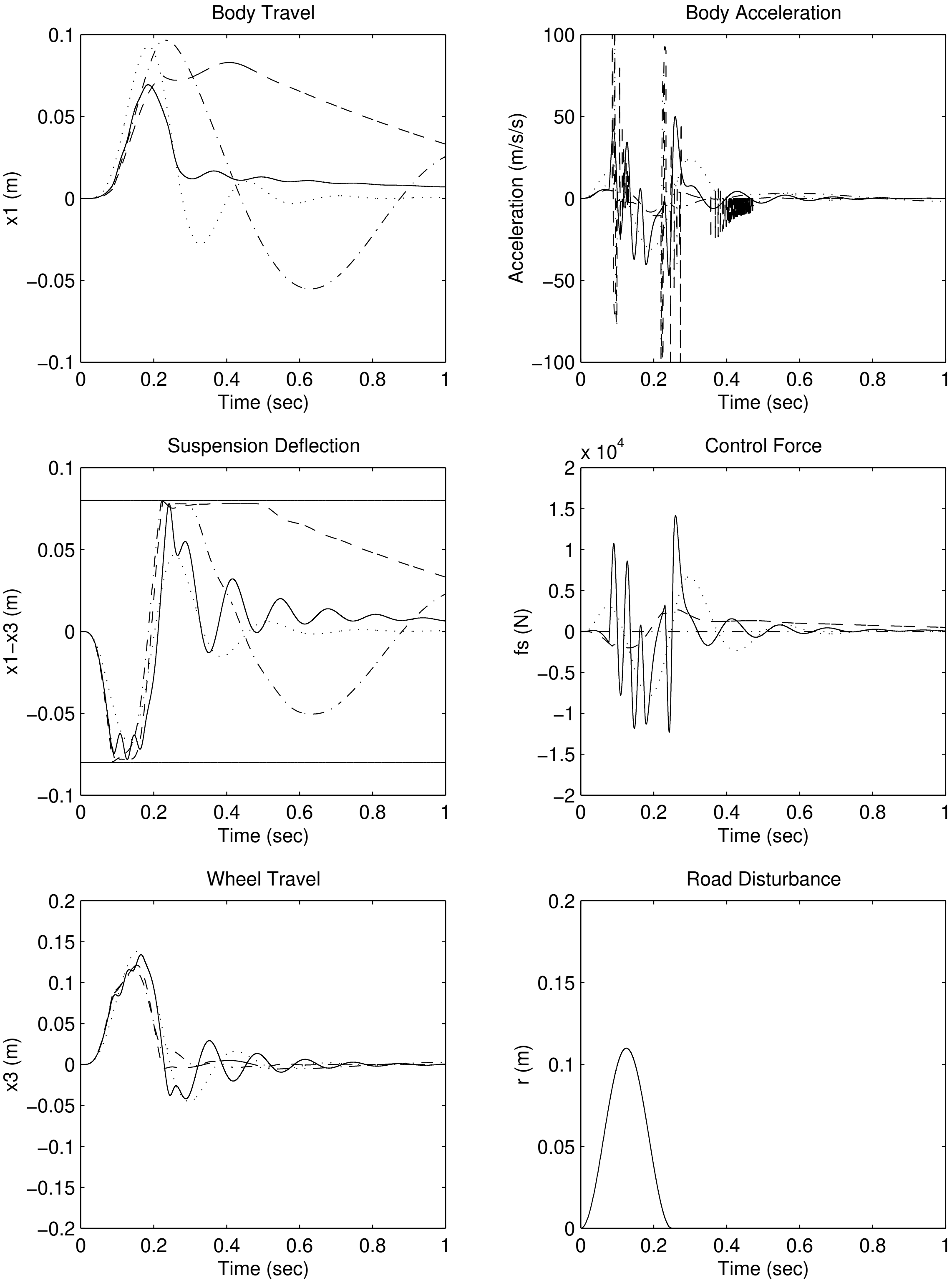

Figure 6: $\mathcal{H}_\infty$ controller responses to a 11 cm bump, Passive (dash-dot), Design 1 (dash), Design 2 (dot), LPV (solid). The solid horizontal lines in the suspension deflection window are the deflection limits.

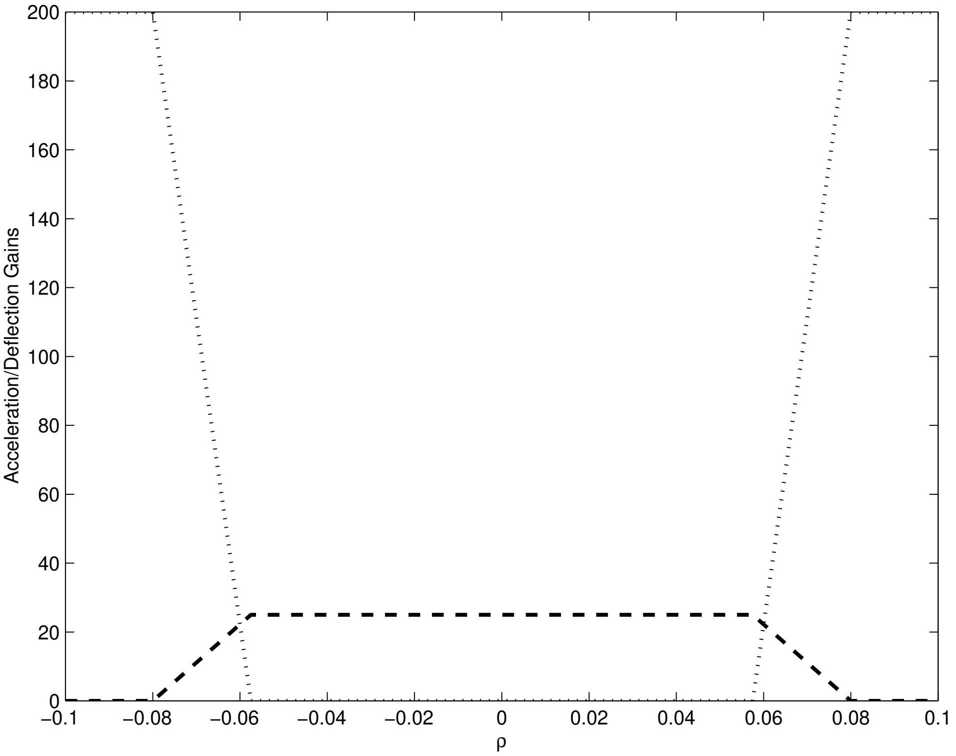

Figure 7: Parameter-dependent gains, $\phi_a[\rho]$ (dash), $\phi_d[\rho]$ (dot)

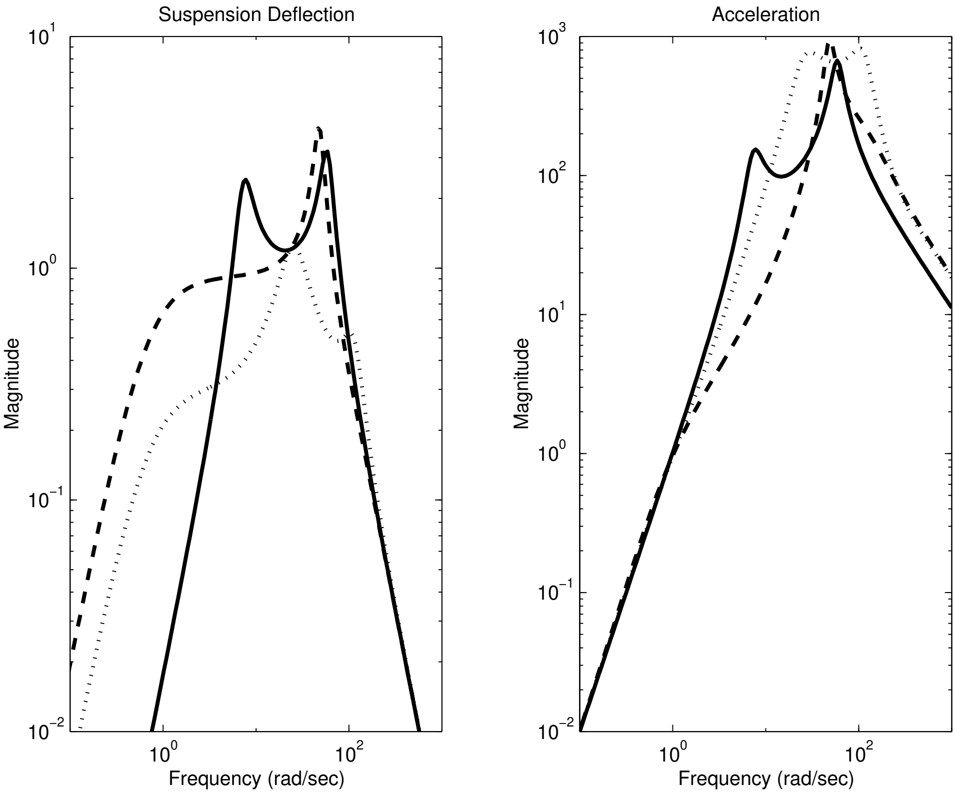

Figure 8: LPV controller: "frozen" closed-loop frequency response, $\rho = 0$ (dash), $\rho = 0.08$ (dot), Passive (solid)

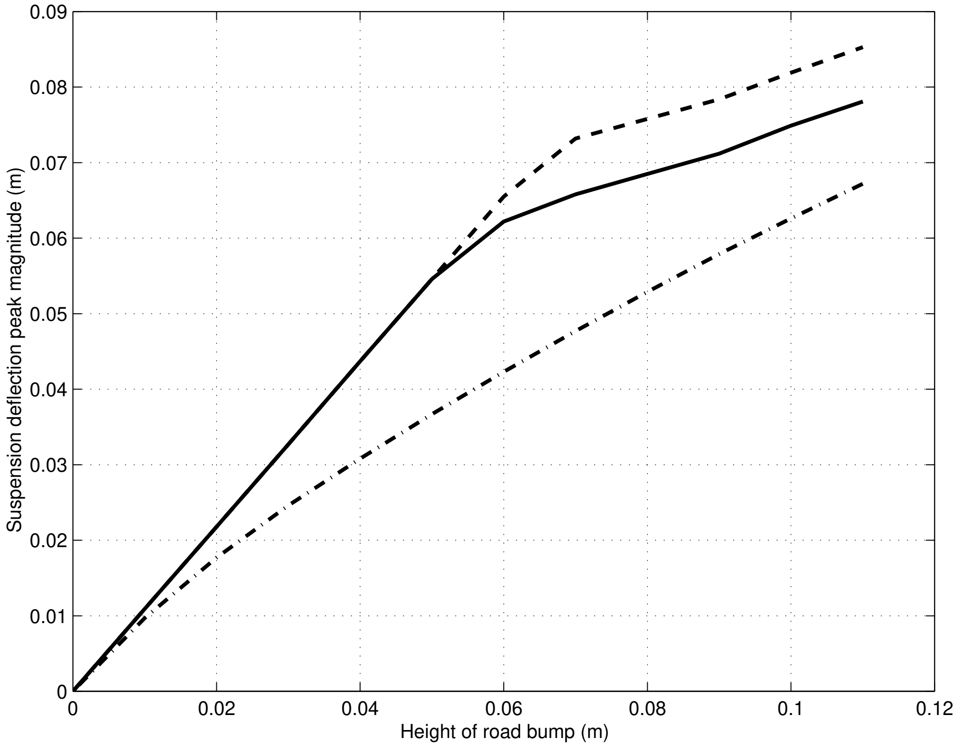

Figure 9: Nonlinear suspension characteristics, $\rho_1 = 0$ (dash-dot), $\rho_1 = 0.0575$ (solid), $\rho_1 = 0.07$ (dash)